Immunization with *Mycobacterium tuberculosis*–Specific Antigens Bypasses T Cell Differentiation from Prior Bacillus Calmette–Guérin Vaccination and Improves Protection in Mice

Claus Aagaard,* Niels Peter Hell Knudsen,* Iben Sohn,* Angelo A. Izzo,† Hongmin Kim,‡ Emma Holsey Kristiansen,* Thomas Lindenstrøm,* Else Marie Agger,* Michael Rasmussen,§ Sung Jae Shin,‡ Ida Rosenkrands,* Peter Andersen,*,¶ and Rasmus Mortensen*

Despite the fact that the majority of people in tuberculosis (TB)–endemic areas are vaccinated with the Bacillus Calmette–Guérin (BCG) vaccine, TB remains the leading infectious cause of death. Data from both animal models and humans show that BCG and subunit vaccines induce T cells of different phenotypes, and little is known about how BCG priming influences subsequent booster vaccines. To test this, we designed a novel *Mycobacterium tuberculosis*–specific (or "non-BCG") subunit vaccine with protective efficacy in both mice and guinea pigs and compared it to a known BCG boosting vaccine. In naive mice, this *M. tuberculosis*–specific vaccine induced similar protection compared with the BCG boosting vaccine. However, in BCG-primed animals, only the *M. tuberculosis*–specific vaccine added significantly to the BCG-induced protection. This correlated with the priming of T cells with a lower degree of differentiation and improved lung-homing capacity. These results have implications for TB vaccine design. *The Journal of Immunology*, 2020, 205: 2146–2155.

Mycobacterium tuberculosis infection is the leading cause of death because of a single infectious agent and has been in the top 10 causes of death worldwide for years (1).The only vaccine currently available against tuberculosis (TB) is *M. bovis* Bacillus Calmette–Guérin (BCG). When administered in early life, BCG efficiently prevents severe forms of childhood TB, but the efficacy against pulmonary disease in adulthood, the most common form of TB disease, is variable (2, 3). Thus, a new vaccine that prevents active pulmonary TB is needed to reduce *M. tuberculosis* transmission and TB-related mortality. CD4 T cells have been shown to be critical for host resistance to *M. tuberculosis* infections and are therefore the most common cell type targeted in preclinical and clinical TB vaccine development (4, 5).

During *M. tuberculosis* infection, Ag expression and presentation have a major effect on differentiation and function of CD4 T cells. Recent mouse studies have shown that TB infection drives the differentiation of *M. tuberculosis*–specific CD4 T cells away from central memory T cells (e.g., secreting IL-2) toward effector/effector memory T cells that predominantly secrete IFN-γ (6). This results in a loss of self-renewing T cell subsets because of an impairment in the IL-2–producing capacity and a reduced capacity to traffic into the infected lung parenchyma (7, 8). Circulating T cells' ability to populate the lung parenchyma has been established as a necessity for T cell–mediated protection in the lung (7, 9), possibly because a direct recognition of infected cells by CD4 T cells via the TCR is required (10). Thus, the ability to resist functional differentiation and home into inflamed lung tissues are key features for long-term protective CD4 T cells (7, 9). Similar to *M. tuberculosis* infection, the live mycobacterial BCG vaccine has been shown to promote differentiation and functional exhaustion of CD4 T cells in parenteral BCG-vaccinated mice, resulting in a failure to efficiently maintain long-term protection

*Department of Infectious Disease Immunology, Statens Serum Institut, DK-2300 Copenhagen, Denmark; †Colorado State University, Department of Microbiology, Immunology and Pathology, Fort Collins, CO 80523; ‡Department of Microbiology, Institute for Immunology and Immunological Diseases, Brain Korea 21 PLUS Project for Medical Science, Yonsei University College of Medicine, Seoul 03722, South Korea; §International Reference Laboratory of Mycobacteriology, Statens Serum Institut, DK-2300 Copenhagen, Denmark; and ¶Department of Immunology and Microbiology, University of Copenhagen, DK-2200 Copenhagen, Denmark

ORCIDs: 0000-0001-6433-3056 (C.A.); 0000-0003-1400-5657 (N.P.H.K.); 0000-0003-3208-2330 (A.A.I.); 0000-0002-9215-2831 (H.K.); 0000-0002-7162-8124 (T.L.); 0000-0002-4401-7598 (M.R.); 0000-0003-0177-3032 (R.M.).

Received for publication May 18, 2020. Accepted for publication August 5, 2020.

This work was supported by The Danish Research Council (DFF - 7016-00310), the National Institutes of Health/National Institute of Allergy and Infectious Diseases (Grant 1R01AI135721-01), the European Union's Horizon 2020 Framework Programme for Research and Innovation under Grant Agreement 643381 as part of the TBVAC2020 Consortium, and the National Institutes of Health/National Institute of Allergy and Infectious Diseases program Advanced Small Animal Models for the Testing of Candidate Therapeutic and Preventative Interventions against Mycobacteria (HHSN272201000009I-003, Task Order 12) at Colorado State University.

Study concept and design, C.A., R.M., P.A., and E.M.A. Experimentation and acquisition of data, N.P.H.K., I.S., E.H.K., M.R., I.R., A.A.I., and H.K. Analysis and interpretation of data, C.A., R.M., P.A., I.R., T.L., E.M.A., A.A.I., and S.J.S. Drafting of the manuscript, C.A. and R.M. Critical and iterative revision of the manuscript and intellectual content, C.A., R.M., and P.A. All authors have reviewed and approved the final manuscript.

Address correspondence and reprint requests to Dr. Rasmus Mortensen, Department of Infectious Disease Immunology, Statens Serum Institut, Region Hovedstaden, DK-2300 Copenhagen, Denmark. E-mail address: rjm@ssi.dk

The online version of this article contains supplemental material.

Abbreviations used in this article: BCG, Bacillus Calmette–Guérin; FDS, functional differentiation score; MIRU, mycobacterial interspersed repetitive unit; TB, tuberculosis.

against *M. tuberculosis* (11–13). A recent study comparing different TB vaccines in clinical testing suggests that BCG may also induce more differentiated T cells than subunit vaccines in people (14). In line with this, we have recently shown that vaccination with an adjuvanted protein subunit vaccine (H56/CAF01) elicits less differentiated CD4 T cells with the capacity to localize to the infected parenchyma (15). In naive animals, such T cells are readily induced, but it has proven difficult to substantially reprogram the immune response after *M. tuberculosis* exposure by subunit vaccination (16–20). Given the similarities between the immune response arising from BCG vaccination and *M. tuberculosis* infection, we hypothesize that pre-existing "BCG-imprinted" T cells dictate the phenotype of the immune response induced by subsequent subunit booster vaccines. To investigate this, we designed two novel vaccines, H64 and H74, that selectively incorporated *M. tuberculosis*–specific (or "non-BCG") Ags and compared the protective efficacy and T cell phenotype to a known booster vaccine sharing all of its Ags with BCG (H65) (21). Thus, H65 was tested as a classical BCG booster vaccine, whereas the H64 and H74 subunit vaccines supplement BCG's Ag repertoire with *M. tuberculosis*–specific Ags. For comparability, the three vaccines consisted of six Ags that were either secreted by or associated with the type VII secretion system (also called the ESX secretion systems). H64 and H74 consisted of ESX-1–associated Ags (*M. tuberculosis* specific), whereas H65 consisted of Ags associated to ESX-2, 3, and 5 (also present in BCG). We first confirmed that the ESX-1 Ags were protective in mice and guinea pigs and that the level of protection was similar to the BCG boosting vaccine H65. We then moved on to show that in BCG-primed mice, the CD4 T cells induced by the H65 booster vaccine were more differentiated than the CD4 T cells induced by the ESX-1–based vaccine. Importantly, the T cells specific for the ESX-1 vaccine maintained their polyfunctionality and low differentiation status during chronic *M. tuberculosis* infection and were superior in entering the *M. tuberculosis*–infected lung parenchyma. As a result, the lung bacterial burden was significantly decreased in the BCG plus ESX-1 vaccination group compared with the groups with either BCG alone or BCG boosted with the H65 vaccine. These data add to the body of evidence supporting the use of ESX-1–associated (or other *M. tuberculosis*–specific/non-BCG) Ags in future TB vaccines (16, 22–25) and address the potential influence of BCG priming on subsequent booster vaccines.

Materials and Methods

Animals

Six- to ten-week-old female mice or 400–500 g outbred female Hartley guinea pigs (Charles River Laboratories) were rested for 1 wk prior to initiation of any experimental procedures. Except for the *M. tuberculosis* Beijing HN878 challenge study, all mouse experiments were performed with female CB6F1 mice (Envigo) at Statens Serum Institut according to the Danish Ministry of Justice and Animal Protection Committees under permit 2014-15-2934-01065 and in compliance with European Union Directive 2010/63/EU. Mice were provided with radiation-sterilized food (Harlan Scandinavia) and water ad libitum and handled in accordance with the Danish Ministry of Justice and Animal Protection Committee regulations by authorized personnel. Infected mice were housed in a biosafety level 3 facility in cages contained within laminar flow safety enclosures (Scantainer, Scanbur). In the challenge study with the hypervirulent *M. tuberculosis* Beijing HN878, female C57BL/6 mice were purchased from SLC (Shizuoka, Japan). All animal experiments were performed according to the Korean Food and Drug Administration regulations and guidelines. The experimental protocols were reviewed and approved by the Ethics Committee and Institutional Animal Care and Use Committee (Permit Number: 2017-0264). All in vivo experiments were carried out under barrier conditions in an animal biological safety level 3 facility at the Avison Biomedical Research Center at Yonsei College of Medicine.

Guinea pigs were maintained under animal biosafety level 3 barrier conditions in isolator cages (Thoren Caging Systems, Hazleton, PA) at Colorado State University. All experimental procedures were conducted in accordance with the Public Health Service Policy on the Humane Care and Use of Laboratory Animals and approved by the Colorado State University Institutional Animal Care and Use Committee (approval no. 13-4565A).

Recombinant proteins

All DNA constructs used in this study were made by chemical synthesis and codon optimized for expression in *Escherichia coli* before insertion into the pJ 411 expression vector (ATUM, Menlo Park, CA). Hybrid H64 and H74 were protein fusions without linkers between the six open reading frames. To minimize protein aggregation, all codons encoding cysteine were replaced with serine codons, five in H74 and three in H64. In both fusions, we added a His tag at the N-terminal end (MHHHHHH-). After transformation into *E. coli* BL21 (DE3) (Agilent Technologies), protein expression was induced with 1 mM isopropyl β-*d*-1-thiogalactopyranoside in 3-l cultures, and the proteins were purified from inclusion bodies by a three-step process as previously described (26). Hybrid H56 and H65 were designed as earlier described (21, 27) and expressed and purified in the same way as H74 and H64. The products were pure full-length products (>99% purity) with a protein concentration between 0.3 and 0.7 mg/ml and a total yield between 4 and 15 mg for the protein batches produced for this work. The identity of all purified protein batches was confirmed by mass spectrometry analysis (matrix-assisted laser desorption/ionization–time-of-flight).

Immunizations and infections

Mice were immunized s.c. three times at 2-wk intervals at the base of the tail with the fusion protein formulated in a cationic liposome adjuvant. Cationic liposomes (CAF01, 250 μg dimethyldioctadecyl-ammonium/50 μg trehalose 6,6-dibehenate) were emulsified with 1–10 μg fusion protein in 10 mM sterile Tris buffer (pH 7.4) to a final volume of 200 μl for each injection. Negative control mice received three equivalent doses of saline, and positive control mice received a single dose of 1×10^5 CFU *M. bovis* BCG Danish 1331 (Statens Serum Institut, Copenhagen, Denmark) given s.c. in the first round of immunization. In *M. bovis* BCG boost experiments, mice received one s.c. injection of 1×10^5 CFU *M. bovis* BCG Danish 1331 and were rested 8–26 wk, depending on the experiment, before vaccination three times with fusion protein as described above. Six weeks after the third immunization, mice were challenged with 50–100 *M. tuberculosis* strain Erdman (American Type Culture Collection), H37Rv (American Type Culture Collection 27294), Kazakhstan (mycobacterial interspersed repetitive units [MIRU] 1270-52), Vietnam (MIRU 1393-252), Beijing (MIRU 94-32), or Beijing HN878 suspended in PBS Tween 20 (0.05%). For *M. tuberculosis* strain Erdman, H37Rv, Beijing, Vietnam, and Kazakhstan, performed at Statens Serum Institut, we used a Biaera exposure system controlled by the AeroMP aerosol management, and for the hypervirulent *M. tuberculosis* strain Beijing HN878 experiment, performed at Yonsei College of Medicine, mice were infected with 60–70 virulent mycobacteria per mouse via the respiratory route using the inhalation chamber (Glas-Col, Terre Haute, IN). Guinea pigs (10/group), housed at Colorado State University, were immunized via the i.m. route and rested for 10 wk. A saline-treated and an intradermal *M. bovis BCG*–vaccinated group (inoculated with 10^3 CFU via the intradermal route) were included as a negative and positive control, respectively. Ten weeks postvaccination, guinea pigs were infected with a low-dose aerosol delivering ~10 viable mycobacteria of virulent *M. tuberculosis* strain H37Rv into the lung of each animal. The animals were euthanized when they reached the set criteria established by the Institutional Animal Care and Use Committee, such as being moribund or exceeding acceptable weight loss and/or being affected in their respiratory rate (labored/heavy breathing). The body temperature was measured to track the clinical progression of the disease. For this, guinea pigs received a s.c. microchip implant (IPT-300 Bio Medic Data Systems, Seaford, DE) that allowed for the measurement of temperature and also carried information about experiment number and animal number. The body temperatures of individual guinea pigs were assessed each day at approximately the same time in the afternoon using a DAS-6006/7 scanner transponder (Bio Medic Data Systems).

Isolation of cells and CFU measurements

Spleen and lymph nodes from individual animals were kept at 4°C until processed through 70-μm nylon cell strainers (BD Pharmingen) followed by two washes and resuspension of the mononuclear cells in RPMI 1640 containing 5% FBS. Isolated lungs were transferred into Miltenyi C tubes containing HEPES/RPMI 1640 supplemented with

collagenase (Roche/Sigma). The lungs were subsequently homogenized and digested for 30–45 min at 37°C and passed through cell strainers (BD Biosciences). After washing, the cells were resuspended in RPMI 1640 containing 5% FBS and stored at 4°C until use. For CFU measurements, lung homogenates were prepared in PBS Tween 80 (0.05%) from individual mice and plated at 3-fold serial dilutions on Middlebrook 7H11 Bacto Agar. After 3 wk of incubation at 37°C, the CFU were enumerated.

Flow cytometry

Single-cell suspensions of splenocytes or lung mononuclear cells (2×10^6 cells/well) were stimulated in vitro in V-bottom 96-well plates at 37°C in 200 μl complete media containing anti-CD49d (1 μg/ml) and anti-CD28 (1 μg/ml) Abs in the presence of rAg (2 μg/ml) for 1 h. Subsequently, 10 μg/ml brefeldin A (Sigma-Aldrich) was added, and the incubation continued for another 5–6 h. Following overnight storage at 4°C, cells were washed in FACS buffer (PBS containing 0.1% sodium azide and 1% FBS) and stained 30 min at 4°C for surface markers with mAbs as indicated. We used 1:400 dilutions of anti-CD4–Brilliant Violet 510 (clone RM 4.5; BioLegend), anti-CD4–Brilliant Violet 786 (clone GK1.5; BioLegend), 1:100 dilutions of anti-CD4–PerCP (clone GK1.5; BioLegend), or 1:200 dilutions of anti-CD4–FITC (clone RM4.4; BD Biosciences) and 1:600 dilutions of anti-CD44–FITC (clone IM7; eBioscience) and anti-CD8–PerCP-Cy5.5 (clone 53-6.7; eBioscience). Cells were then washed in FACS buffer, permeabilized using the Cytofix/Cytoperm kit (BD Biosciences) according to the manufacturer's instructions, and stained intracellularly for 30 min at 4°C in dilutions of 1:200 using anti–IFN-γ–PE-Cy7 or anti–IFN-γ–PerCP-Cy5.5 (clone XMG1.2; eBioscience), anti–TNF-α–PE or anti–TNF-α–PeCy7 (clone MP6-XT22; eBioscience), anti–IL-17–allophycocyanin (clone eBio17B7; eBioscience), or dilutions of 1:100 using anti–IL-2–allophycocyanin-Cy7 (clone JES6-5H4; BD Biosciences) mAbs. Cells were subsequently washed with BD Perm/Wash Buffer (BD Biosciences) and resuspended in FACS buffer. Data were collected by running the stained cells on a FACSCanto, FACSCalibur, or FACSFortesa flow cytometer (BD Biosciences) and analyzed using FlowJo software v.10.0.7.

In vivo intravascular labeling of T cells

At the day of the experiment, mice were injected i.v. with 2 μg of FITC-labeled Abs against CD45.2 in a total volume of 200 μl (clone 102; BioLegend, San Diego, CA). Three minutes after Ab injection, mice were euthanized, and single-cell suspensions were prepared as described above.

Adoptive transfer and lung homing

For coadoptive transfer studies, donor CD4 T cells from subunit-vaccinated and *M. bovis* BCG plus subunit–vaccinated animals were isolated by negative selection 3 wk after the last immunization. In brief, cells were isolated from spleen, medial iliac, inguinal, and axillary lymph nodes from eight individual vaccinated donor animals, pooled within the groups and enumerated. Untouched CD4 T cell enrichment was performed from 5×10^8 cells per group using the EasySep Mouse CD4 T cell Enrichment Kit following the manufacturer's instructions (STEMCELL Technologies). After enrichment, cells were counted, and the density was adjusted to 2.5×10^7 cells per ml for each group (93–95% purity). For tracking, the purified cells were differentially stained for 10 min with 10 μM Cell Proliferation Dye eFluor 450 or 5 μM Cell Proliferation Dye eFluor 670 (Thermo Fisher Scientific). The proliferation dyes were quenched with PBS containing 20% FBS followed by washing and resuspension in PBS. Stained cells were mixed in a ~1:1 ratio and coadoptively transferred into recipient mice that were infected with *M. tuberculosis* strain Erdman 3 wk prior. Two hundred microliters (5×10^6 CD4 T cells) was injected into the lateral tail vein of individual recipient mice (the equivalent of one donor mouse per recipient mouse). Eighteen hours after transfer, recipient mice were injected with FITC-labeled anti-CD45.2 Abs for intravascular labeling (clone 102; BD Biosciences) and single-cell suspensions from the lung prepared as described above.

Statistical analysis

Prism 7 software (GraphPad Prism ver. 8.2.1, San Diego, CA) was used for all statistical analyses. Mean and SEM are indicated for log-transformed CFU counts. Mean and SD are indicated for immune responses. One-way ANOVA combined with Tukey multiple comparison test was used for comparing multiple groups. Statistical significant differences are indicated by asterisks in the figures: $*p < 0.05$, $**p < 0.01$, $***p < 0.001$, and $****p < 0.0001$. In the guinea pig experiment, the nonparametric log-rank test was used to compare the survival distributions of two samples comparing the survival curves for the vaccinated groups against the saline group.

Results

ESX-1–associated Ags (M. tuberculosis–specific) provide protection in mice and guinea pigs

To investigate the influence of BCG priming on subsequent subunit vaccination, we first designed protective subunit vaccines that selectively incorporated *M. tuberculosis*–specific Ags, which are not shared with BCG. The *M. tuberculosis* genome encodes ~4000 proteins, of which many are potential vaccine targets. However, ~3900 of these have highly similar orthologs in the BCG genome, which significantly limits the number of potential Ags for this type of vaccine (28, 29). In our selection, we exploited that all BCG substrains lack the genomic locus "region of difference 1" (23), which includes the core genes for the ESX-1 secretion system. In virulent *M. tuberculosis* strains, ESX-1–secreted proteins are among the most immunogenic Ags and are frequently recognized in TB patients and latently infected individuals (30, 31). However, in BCG, the region of difference 1 deletion is expected to prevent priming of T cells against ESX-1–associated Ags, and we therefore selected among this group of proteins for the first subunit vaccine, referred to as H64. We selected six ESX-1–associated Ags for which proteome studies had identified the proteins in *M. tuberculosis* culture filtrate or membrane fractions (Table I) and constructed the H64 subunit vaccine as a recombinant fusion protein (Fig. 1A). In H64-vaccinated CB6F1 mice, the CD4 T cells recognized the EsxA, EspD, and EspR Ags (Fig. 1B), and we found that the subunit vaccine induced protection with protein doses ranging from 0.01 to 25 μg per vaccination peaking in the range of 1–5 μg (Fig. 1C). Based on this, an intermediate dose of 2 μg was selected for future mouse studies. Because disease progression and granuloma formation in *M. tuberculosis*–infected guinea pigs better mimic features of human TB pathology, we also tested the H64 vaccine in Hartley guinea pigs in a long-term infection model. Guinea pigs were challenged with a low dose of virulent *M. tuberculosis* H37Rv after vaccination with different doses of H64. Animals that reached predefined human end points (weight loss or impact on respiratory rate) were euthanized. Twenty-two weeks after being infected, all animals in the saline control group had been euthanized with a mean survival time of 16.2 wk (SD = ±1.8) (Supplemental Fig. 1A). In comparison, the mean survival time of the *M. bovis* BCG-vaccinated guinea pigs was 65.1 wk (±8.9). In the four H64-vaccinated groups, the mean survival time ranged from 22.4 wk (±2.3) to 41.6 wk (±9.0) (Fig. 1C). Statistical comparison confirmed that all vaccination groups were better protected than saline-vaccinated animals ($p < 0.02$, log-rank test). After having confirmed that the ESX-1–associated Ag combination was protective in both mice and guinea pigs, we continued our study of the H64 vaccine by testing its protective efficacy against different challenge strains. Because *M. tuberculosis* strains harbor genetic diversity that translates into significant differences in Ag diversity, immunogenicity, and virulence, we selected four clinically relevant *M. tuberculosis* strains belonging to different lineages (2–4) to ensure that the protective signal of H64 was robust and broadly relevant (Fig. 1D, Supplemental Fig. 1B) (32). Similarly to the results with *M. tuberculosis* Erdman in Fig. 1C, H64 vaccination induced significant protection against all four strains ($p < 0.05$ or lower) and was equal to or better than the protection obtained with the H56 subunit vaccine that was included to benchmark the new vaccine. In the experiment with H37Rv,

Table I. *M. tuberculosis* Ags in the H64 fusion protein

H37Rv Number	Name	Size (Amino Acid)	Reference[a]
Rv3865	EspF	103	(59, 60)
Rv3872	PE35	99	(60)
Rv3615c	EspC	103	(59, 60)
Rv3614c	EspD	184	(59, 60)
Rv3875	EsxA	95	(59, 60)
Rv3849	EspR	132	(59, 60)

[a]Protein identified in membrane fraction or culture filtrate.

H64 was more protective than BCG, but with the other clinical strains, BCG induced similar or better protection than H64 (Fig. 1D). To test how the vaccine performed against a more "aggressive" strain, we challenged mice with *M. tuberculosis* HN878, which is regarded as hypervirulent because of its rapid growth and induction of severe lung inflammation in mice (33). In this model, both BCG and H64 protected efficiently at week 4 of the infection ($p < 0.001$), but by week 12, BCG had lost most of its protection, whereas bacterial numbers in H64-vaccinated animals remained significantly lower than BCG as well as the saline control (Fig. 1E, $p < 0.005$ and $p < 0.0001$, respectively).

In parallel to working with H64, we designed an additional ESX-1 fusion protein in which EspF and PE35 (not immunogenic in H64) were replaced with the Ags EspB and EspA to potentially optimize immunogenicity and/or efficacy (Fig. 2A, Table II). In H74-vaccinated animals, there was a dominant CD4 T cell response to EspB and an increased recognition of EsxA and EspD (Fig. 2B). Similar to H64, H74 induced protective efficacy over a broad range of vaccination doses peaking between 1 and 5 μg (Supplemental Fig. 1C). Because both vaccines were designed to be used in BCG-primed animals, we did a direct head-to-head comparison in this setting. After challenge with *M. tuberculosis* Erdman, both vaccines induced robust protection on top of BCG at all the measured time points (Fig. 2C). However, at the late time point (20 wk postinfection), lung bacterial numbers were reduced by 1.7 $\log_{10}$ in the BCG control group ($p < 0.0001$), 1.88 $\log_{10}$ in the BCG-H64–vaccinated group, and 2.22 $\log_{10}$ in the BCG-H74–vaccinated group compared with the saline group. The bacterial burden was thus significantly lower in the H74-vaccinated animals ($p < 0.01$), and H74 was selected as the ESX-1 vaccine for further studies.

In summary, we designed two novel vaccines based exclusively on ESX-1–associated Ags H64 and H74 which demonstrated robust protection in both mice and guinea pigs. H74 was selected for further studies in BCG-primed animals.

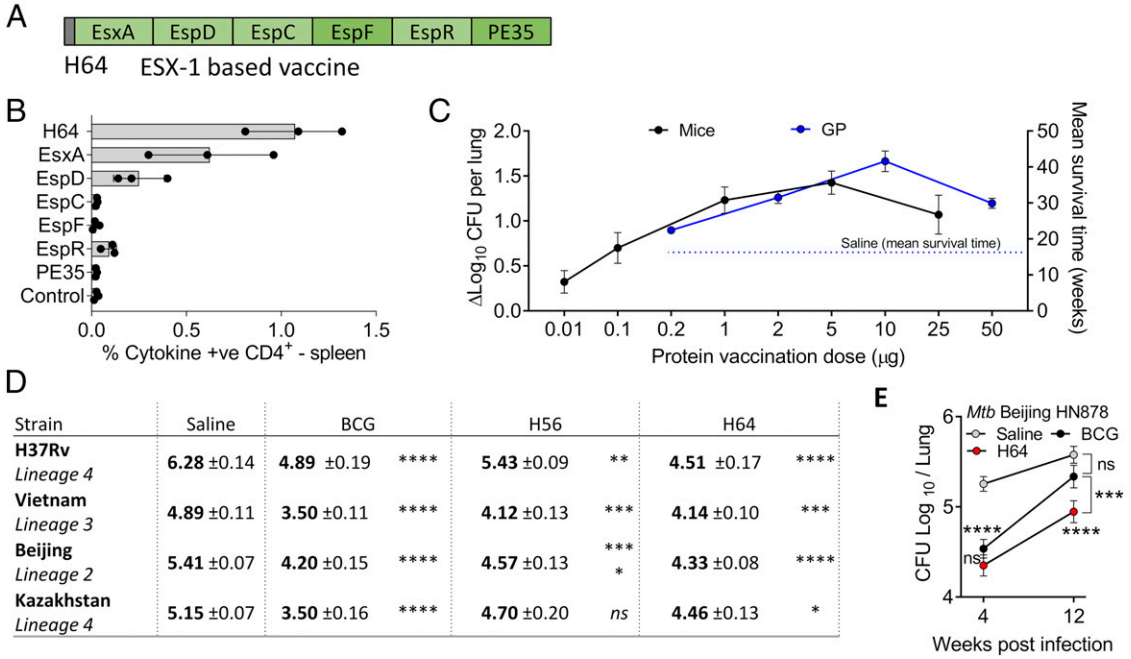

Strain	Saline	BCG		H56		H64	
H37Rv *Lineage 4*	**6.28** ±0.14	**4.89** ±0.19	****	**5.43** ±0.09	**	**4.51** ±0.17	****
Vietnam *Lineage 3*	**4.89** ±0.11	**3.50** ±0.11	****	**4.12** ±0.13	***	**4.14** ±0.10	***
Beijing *Lineage 2*	**5.41** ±0.07	**4.20** ±0.15	****	**4.57** ±0.13	*** *	**4.33** ±0.08	****
Kazakhstan *Lineage 4*	**5.15** ±0.07	**3.50** ±0.16	****	**4.70** ±0.20	*ns*	**4.46** ±0.13	*

FIGURE 1. H64 (ESX-1–associated Ags) provide protection against *M. tuberculosis* in mice and guinea pigs. (**A**) Illustration of the subunit vaccine H64. The fusion protein is based on ESX-1–associated Ags and does not share Ags with *M. bovis* BCG. The figure is not drawn to scale. The m.w. of the individual Ags is given in Table I. (**B**) Ag recognition of splenocytes after immunizing CB6F1 mice with H64 ($n = 3$). Single-cell cytokine expression was measured by flow cytometry. Any CD4 cell that produced either IFN-γ, TNF-α, and/or IL-2 in response to Ag stimulation was taken as Ag specific. The spleen cells were stimulated with single Ags from H64. EsxH stimulation was included as a negative control ("Control"). Bars and lines illustrate the mean and SD for each Ag. (**C**) Black curve: protective efficacy studies in CB6F1 mice. Animals were immunized with different doses of H64 in CAF01 adjuvant. The bacterial load was measured in lungs from individual mice 6 wk after *M. tuberculosis* Erdman challenge ($n = 8$). The number of bacteria was logarithmic transformed and subtracted from the bacteria numbers in a nonvaccinated control group. Blue curve: protective efficacy studies in guinea pigs (performed at Colorado State University). Guinea pigs were immunized with different doses of H64 in CAF01 and euthanized when predefined humane end points were met after *M. tuberculosis* infection. Kaplan–Meier survival curves (Supplemental Fig. 1A) were used to estimate the mean survival time for guinea pigs in each of the vaccination groups ($n = 10$). SDs are shown for each data point. (**D**) CB6F1 mice immunized with H64, H56, or *M. bovis* BCG or injected with saline were infected for 6 wk with one of four clinical isolates of *M. tuberculosis:* H37Rv, Vietnam, Nepal, and Kazakhstan ($n = 6$–8 per group). MIRU typing in Supplemental Fig. 1B. CFU Log_{10}/lung ± SEM. One-way ANOVA was used for statistical comparison with the saline group for each strain; degree of freedom = 24. (**E**) H64 or *M. bovis* BCG immunized or saline-injected C57BL/6 mice were infected 6 wk after immunization with the hypervirulent *M. tuberculosis* strain Beijing HN878 (performed at Yonsei College of Medicine). After 4- and 12-wk infection, the bacterial burden was measured in the lung ($n = 5$–8). Mean values and SEMs are illustrated. One-way ANOVA was used for statistical comparison between groups for each time point; degree of freedom = 18. *$p < 0.05$, **$p < 0.01$, ***$p < 0.001$, ****$p < 0.0001$.

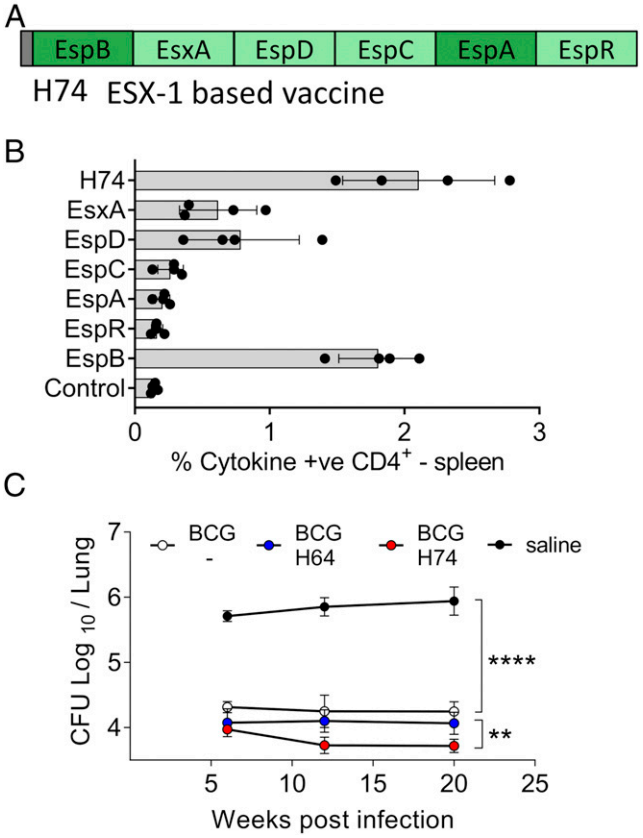

FIGURE 2. Improved Ag recognition and protection of H74 compared with H64. (**A**) Illustration of the subunit vaccine H74. The fusion protein is based on ESX-1–associated Ags. Ags shared with H64 are in light green. The length in amino acids of the individual Ags is given in Table I. (**B**) Ag recognition of splenocytes isolated from H74-immunized CB6F1 mice (n = 4). The cells were stimulated with single Ags from H74, and EsxH stimulation was included as negative control (Control). CD4 T cells producing either IFN-γ, TNF-α, and/or IL-2 in response to Ag stimulation were taken as Ag specific. Means and SDs are shown for each Ag. (**C**) Six months after being *M. bovis* BCG–vaccinated, CB6F1 mice were divided into three groups and vaccinated with either H64 or H74 or saline injected. An age-matched control group was included that did not receive any of the vaccines. All animals were aerosol infected with *M. tuberculosis* Erdman, and the number of mycobacteria was measured in individual lungs from immunized and nonimmunized mice 6, 12, and 20 wk postinfection (n = 8 per time point). Vertical lines illustrate SEMs. One-way ANOVA was used for statistical comparison between groups at the late time point; degree of freedom = 28. $^{**}p < 0.01$, $^{****}p < 0.0001$.

In BCG-vaccinated mice, ESX-1–associated Ags induce less differentiated CD4 T cells and improve protection compared with BCG boosting

It has been demonstrated that BCG vaccination induces highly differentiated T cells (34), but it has not been systematically investigated how this influences T cell quality and protection of subsequent subunit vaccine boosters. We approached this issue by first comparing the protective efficacy of the ESX-1–based H74 vaccine and a BCG booster vaccine (H65), described in a previous study (21). H65 consists of six EsxA family proteins related to ESX-2, -3, or -5 that are all present in BCG (Fig. 3A). Naive mice were immunized with either H65 or H74 as standalone vaccines. Six weeks after *M. tuberculosis* aerosol challenge, both vaccines reduced the bacterial load by more than 1.0 $\log_{10}$ relative to nonvaccinated animals ($p < 0.0001$) with no statistical difference between them (Fig. 3B). Having confirmed that the two vaccines induced similar levels of protection in naive mice, we continued by comparing their efficacy in mice that were BCG primed 6 mo prior to subunit vaccination. Twelve weeks after *M. tuberculosis* Erdman challenge, BCG vaccination reduced the lung bacterial number by 0.85 $\log_{10}$ ($p < 0.05$). In two separate experiments, H65 boosting did not add significantly to this protection (Fig. 3C, top, Supplemental Fig. 2A), whereas vaccination with the H74 vaccine enhanced the BCG-induced protection ($p < 0.05$), resulting in a 1.78 $\log_{10}$ reduction of the number of bacteria relative to the nonvaccinated group ($p < 0.0001$). This observation was robust as similar results were found in a second study with the clinical strain *M. tuberculosis* Kazakhstan (Fig. 3C, bottom), showing consistently that although the protection was equal in naive mice, the ESX-1 vaccine (*M. tuberculosis*–specific) induced better protection than the BCG boosting vaccine in BCG-primed animals.

Table II. *M. tuberculosis* Ags in the H74 fusion protein

H37Rv Number	Name	Size (Amino Acid)	Reference[a]
Rv3615c	EspC	103	(59, 60)
Rv3614c	EspD	184	(60)
Rv3875	EsxA	95	(59, 60)
Rv3849	EspR	132	(59, 60)
Rv3616c	EspA	392	(59, 60)
Rv3881c	EspB	460	(59, 60)

[a]Protein identified in membrane fraction or culture filtrate.

Next, we compared the phenotype of the subunit-specific CD4 T cell response among the vaccinated groups before and after *M. tuberculosis* challenge (Fig. 3D). We used the individual CD4 T cell cytokine expression profile as a specific and sensitive measure to assess the degree of differentiation (35). For each group, we calculated a simple functional differentiation score (FDS) based on the ratio of IFN-γ producers and nonproducers as has previously been suggested (6). In BCG-vaccinated animals, we found the highest degree of T cell differentiation (FDS = 4.0) with the majority of responding CD4 T cells expressing IFN-γ either alone or in combination with TNF-α and/or IL-2 (Fig. 3E, top). In the H65-boosted group, there was almost a 3-fold increase in the percentage of H65-specific CD4 T cells compared with BCG alone, but H65 boosting induced only minor changes in the cytokine expression profile of the CD4 T cells (FDS = 2.8, Fig. 3E, middle). In contrast, H74 vaccination induced CD4 T cells with a lower degree of differentiation with almost half of the responding T cells expressing TNF-α alone or TNF-α and IL-2 in combination (FDS = 1.0, Fig. 3E, bottom). After *M. tuberculosis* Erdman infection, the CD4 T cells recruited to the lung maintained an FDS score of ∼ 4.0 in BCG-vaccinated mice during the initial phase of the infection. However, this increased to 10.7 after 6 wk and to 26.1 after 12 wk of infection, clearly showing a further differentiation of the T cell pool during TB infection (Fig. 3F, top). In the H65-boosted group, there was a delay in the differentiation of the CD4 T cells, but at the late time point, the FDS score had increased to 12.8 (Fig. 3F, middle). In contrast, the FDS score for the vaccine-specific CD4 T cells remained around ∼1.0 for all time points in the H74-vaccinated group (Fig. 3F, bottom). Thus, the pool of H74-specific CD4 T cells effectively resisted infection-driven differentiation throughout a 12-wk infection period. We further investigated this in a follow-up study, in which BCG-primed animals were immunized simultaneously with H74 and H65 so that each animal served as its own internal control. In these animals, the H65-specific CD4 T cells had a mean FDS of 3.0 compared with 0.84 for the H74-specific CD4 T cells, confirming that BCG boosting leads to higher T cell differentiation than vaccination with *M. tuberculosis*–specific

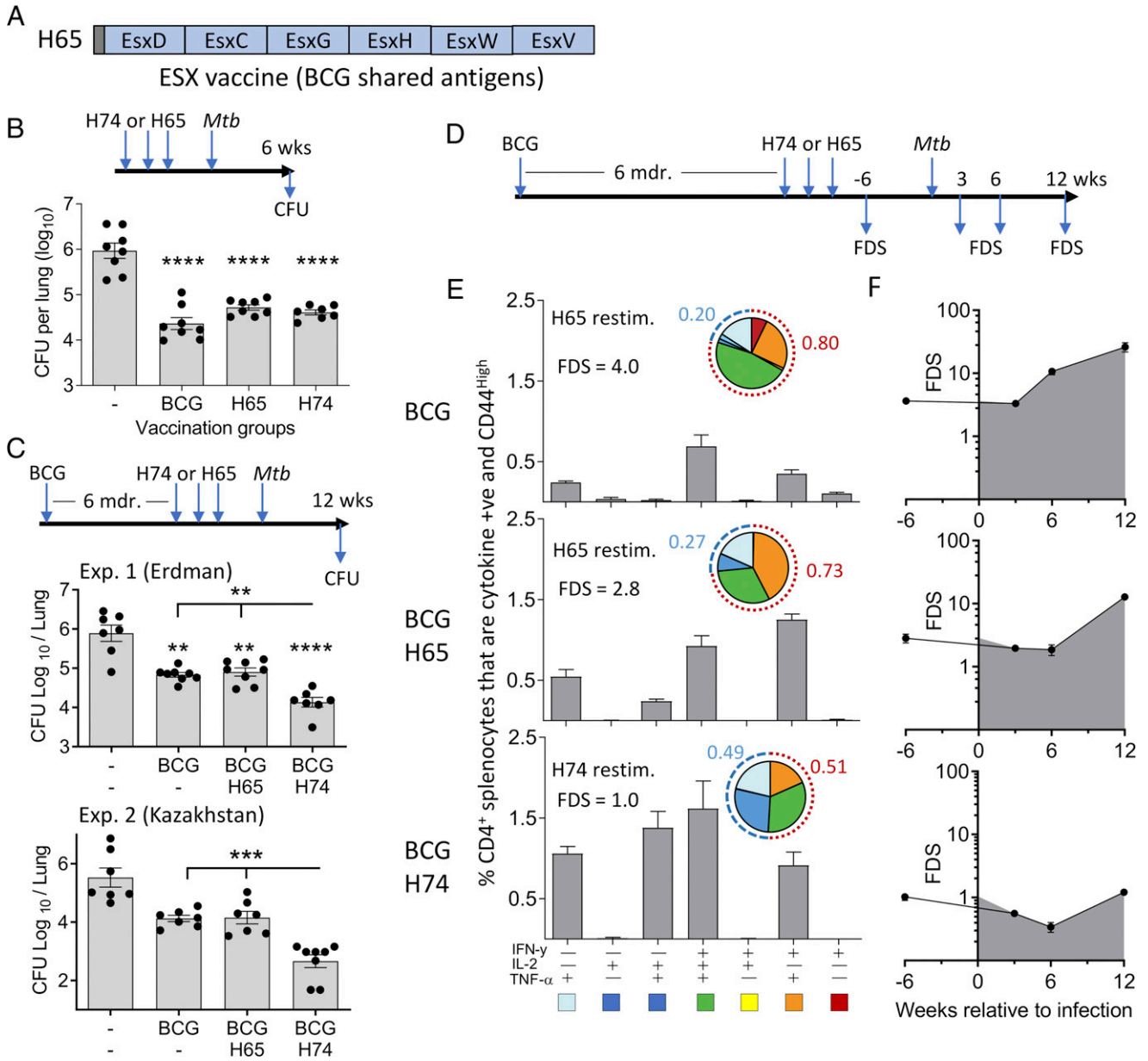

FIGURE 3. H74 vaccination (ESX-1–associated Ags) improve protection in BCG-primed animals and induce less differentiated CD4 T cells compared with BCG boosting (H65). (**A**) Illustration of the BCG booster vaccine H65. All six Ags are shared with *M. bovis* BCG (21). (**B**) Groups of naive CB6F1 mice were vaccinated with H74 or H65, and control groups received either a BCG vaccination or saline injections ($n = 8$). The bacterial numbers were enumerated in lungs 6 wk after an aerosol *M. tuberculosis* Erdman infection. Means and SEMs are shown by bars and lines. One-way ANOVA was used for statistical analysis; degree of freedom = 27. (**C**) CB6F1 mice were BCG vaccinated followed by a resting period of 6 mo before being vaccinated with either H74 or H65 ($n = 7$–8). The bacterial numbers were measured in individual animals 12 wk after they were infected with *M. tuberculosis* strain Erdman (top) or 25 wk after *M. tuberculosis* Kazakhstan infection (bottom). One-way ANOVA was used for statistical analysis; degree of freedom = 25 and 26. (**D**) Timeline for measuring T cell responses in vaccinated CB6F1 mice pre– and post–*M. tuberculosis* Erdman challenge in the BCG prime–boost model. (**E**) Splenocytes isolated from CB6F1 mice vaccinated with BCG alone or boosted with H65 were stimulated with the H65 fusion protein. In parallel, splenocytes from BCG-vaccinated animals complemented with H74 were stimulated with the H74 fusion protein. Single-cell expression of cytokine IFN-γ, TNF-α, and IL-2 was measured by flow cytometry, and the frequencies of activated ($CD44^{high}$) CD4 T cells expressing any of the possible combinations of cytokines are shown in a bar plot for each vaccination group with mean and SD indicated ($n = 3$). Means (gray bars) and SDs (vertical lines) are shown. The pies are a simplified view of the data illustrating cytokine coexpression patterns of the specific CD4 T cells. The five identified subgroups of cytokine-producing CD4 T cells were as follows: light blue, TNF-α^+; dark blue, TNF-α^+ and IL-2^+; green, TNF-α^+, IL-2^+, and IFN-γ^+; orange, IFN-γ^+ and TNF-α^+; and red, IFN-γ^+. The dotted arches illustrate the fraction of specific CD4 T cells that produced IFN-γ (red) or did not produce cytokine IFN-γ (blue) in response to ex vivo Ag stimulation. The FDS was calculated as the ratio of IFN-γ producers/IFN-γ nonproducers as previously described (6). (**F**) Cytokine expression profiles were measured in spleens before and in lungs after *M. tuberculosis* Erdman infection, and the associated FDS score was calculated for each time point and vaccination group ($n = 3$–4 per time point). Filled circles and vertical bars represents means and SDs. $^{**}p < 0.01$, $^{***}p < 0.001$, $^{****}p < 0.0001$.

Ags (Supplemental Fig. 2B). Finally, ESAT-6 has been shown to be essential for postexposure protection (16), and of relevance to the vaccination of *M. tuberculosis*–exposed individuals, H74 vaccination induced less differentiated T cells and lower bacterial burdens in the modified Cornell model of latent TB infection, supporting ESX-1–based vaccines for this application (27, 36) (Supplemental Fig. 2C).

In summary, in BCG-primed mice, H65 vaccination did neither lead to substantial improvements in T cell differentiation nor did it add significantly to the protection induced by BCG. Conversely, vaccination with ESX-1–associated Ags (H74) induced CD4 T cells with a low differentiation score, which remained low during *M. tuberculosis* infection. This correlated with a significantly increased protective efficacy.

In BCG-vaccinated mice, ESX-1–associated Ags induce CD4 T cells with superior lung-homing capacity

Recent studies directly link T cell differentiation status to the ability to enter the infected lung parenchyma and restrict mycobacterial growth (7, 9, 15, 37). In H56/CAF01-vaccinated mice, we have previously shown that lung parenchymal CD4 T cells (protected from anti-CD45 i.v. stain) are less differentiated and express increased levels of the parenchymal homing marker, CXCR3 (15). For this study, to directly link FDS with lung parenchymal trafficking, we first confirmed that there was a strong correlation between FDS and i.v. CD45 labeling in vaccinated animals (Supplemental Fig. 3).

Because our data this far showed that pre-existing BCG immunity had a major influence on the differentiation status of subunit-specific CD4 T cells, we next investigated the impact of BCG boosting on lung-homing capacity. For this, we performed an adoptive transfer experiment using donor cells from H74- and H65-vaccinated mice with or without BCG priming. Before cell transfer, we confirmed that all four groups had a solid vaccine-specific CD4 T cell response and used the cytokine expression profiles to determine the degree of CD4 T cell differentiation (Fig. 4A, 4B). Importantly, the T cell differentiation was similar after H74 and H65 vaccination when administered as standalone vaccines, confirming there was no inherent difference in the priming capability of these vaccines. However, in BCG-primed mice, H65 boosting led to a higher T cell differentiation than H74 vaccination, as previously observed (Fig. 4B).

To compare the ability of the vaccine-specific CD4 T cells to enter infected lung parenchyma, we transferred mixed populations of CD4 T cells into *M. tuberculosis*–infected recipients. Donor CD4 T cells from the four vaccination groups were isolated by negative selection from spleens and inguinal lymph nodes and stained either with Cell Proliferation Dye eFluor 450 or Cell Proliferation Dye eFluor 670 to distinguish cells from BCG-primed animals and cells from animals receiving the subunit vaccine as a standalone. Stained cells were mixed in a ~1:1 ratio (subunit:BCG prime plus subunit) and cotransferred into *M. tuberculosis* Erdman–infected recipients in a total 5×10^6 donor CD4 T cells per recipient. Eighteen hours after transfer, recipient mice were injected with FITC-labeled anti-CD45.2

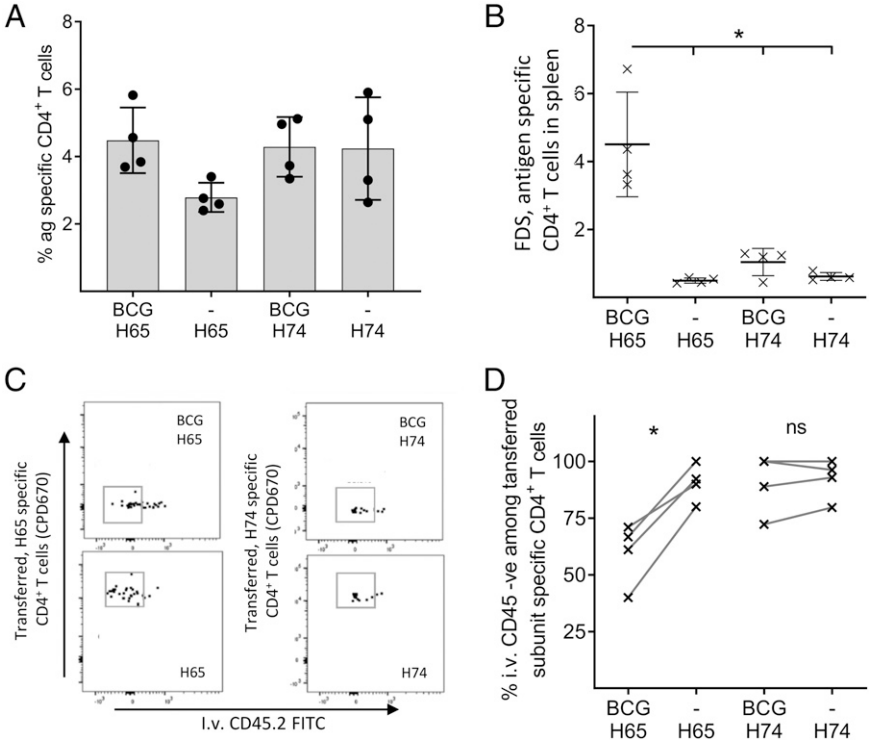

FIGURE 4. H74 (ESX-1–associated Ags) induces CD4 T cells with superior lung-homing capacity in BCG-vaccinated mice. (**A**) Eight weeks after being BCG vaccinated, CB6F1 mice were vaccinated with H65 or H74. Three weeks later, splenocytes were stimulated with H65 or H74 fusion protein, and the expression of cytokines IFN-γ, IL-2, and TNF-α was measured by flow cytometry. CD4 T cells that produced at least one of the cytokines in response to Ag stimulation was regarded as "Ag specific" ($n = 4$ per group). The mean (gray bar) and SD is shown for each group. (**B**) The FDS score was calculated as the ratio of IFN-γ^+/IFN-γ^- cells based on the cytokine expression profile for the individual animal and plotted for each of the four vaccination groups. Horizontal lines represent means, vertical lines, and SDs. One-way ANOVA was used for statistical comparison; degree of freedom = 12. (**C**) The influence of BCG priming on the lung-homing capacity of H65- and H74-induced CD4 T cells. CD4 T cells were purified from spleens and lymph nodes and pooled within the vaccination groups before labeling with tracker dyes to distinguish cells from donor animals with and without BCG priming. After labeling, cells were mixed 1:1 (e.g., naive plus H65:BCG plus H65) and adoptively transferred to *M. tuberculosis* Erdman–infected mice. The next day, intravascular localized cells in the recipient mice were labeled using FITC CD45.2, and purified lung cells were stimulated with fusion proteins to identify cytokine expressing ("Ag-specific") CD4 T cells. For the entire gating strategy, see Supplemental Fig. 4. (**D**) For each of the four vaccination groups, the percentage of vaccine-specific donor cells entering into the lung parenchyma was calculated, and the influence of BCG priming on vaccine-specific homing was compared for the two subunit vaccines. The lines connect measurements from the same recipient mouse ($n = 4$). The statistical comparison was done by two-tailed t tests. *$p < 0.05$.

for intravascular labeling, and lung cells were harvested for flow cytometric analysis based on CDP450/670 as well as cytokine staining following H65/H74 stimulation (Fig. 4C, Supplemental Fig. 4). In mice receiving H65-specific cells, only 39.6–72.0% (mean 64%) of the cells from the BCG-H65–boosted donor mice were located in the lung parenchyma, whereas the range was 79.3–99.4% (mean 90%) for donor cells from H65-only vaccinated mice (Fig. 4D). In contrast, we found no significant differences in the percentage of H74-specific CD4 T cells in the parenchyma regardless of whether the cells came from H74 only or BCG-H74–vaccinated animals (range 78.0–99.4 and 72.0–99.4%, respectively, with means of 85.0 and 84.2%).

These results clearly demonstrate that pre-existing BCG immunity significantly impacts the functionality of the T cells induced by subunit booster vaccines and that this mechanism can be efficiently bypassed by designing vaccines that selectively incorporate BCG-complementing TB Ags.

Discussion

The capacity of CD4 T cells to protect against *M. tuberculosis* is governed by their differentiation state and ability to localize to the site of infection (37). *M. bovis* BCG vaccination primes a polyfunctional CD4 T cell response that differentiates over time and gradually loses the ability to produce IL-2, proliferate, and to localize to the site of infection, which results in a loss of long-term protective efficacy (11–13). Heterologous prime–boost strategies, in which BCG vaccination is followed by a subunit vaccine boost, are aiming at improving the BCG-induced adaptive immunity in terms of magnitude, durability, and quality of the CD4 T cell response (38). In this study, we tested whether pre-existing BCG immunity impacts the vaccine response of either a "traditional" BCG booster vaccine (H65) or a complementary vaccine based on ESX-1–associated Ags that are specific for *M. tuberculosis* (H74 and H64, referred to collectively as "ESX-1 vaccines").

In the initial characterization of the ESX-1 vaccines, we demonstrated significant long-term protection in *M. tuberculosis* H37Rv–challenged guinea pigs as well as *M. tuberculosis* Erdman–challenged mice. To extend the study beyond the conventional laboratory *M. tuberculosis* strains, we challenged vaccinated mice with four different strains of *M. tuberculosis* belonging to three phylogenetically different lineages. The ESX-1 vaccine induced significant protection against all four strains, suggesting that the vaccine will be effective against a broad range of clinical isolates. Two of the selected isolates were part of the W-Beijing family of *M. tuberculosis* strains, one of them being the hypervirulent *M. tuberculosis* Beijing HN878. The Beijing strains are particularly relevant to include in this screening as they are highly prevalent, overrepresented among drug-resistant isolates (39), and significantly associated with HIV coinfection in human cases of TB meningitis (40). In a conventional protection readout at 4 wk postinfection, both the ESX-1 vaccine and BCG were highly protective against *M. tuberculosis* Beijing HN878. This was also true at the later time point for the ESX-1 vaccine, but in line with earlier studies (27, 41), BCG's protective efficacy waned at the later stage of infection.

In the prime–boost model, our data indicates that BCG vaccination has a major influence on the immune responses induced by subsequent subunit vaccines, depending on whether the Ags are shared with BCG or not. Specifically, we observed that boosting BCG with H65 only marginally changed the specific CD4 T cell differentiation status with little or no improvement of the protection. In contrast, BCG priming had minimal influence on the differentiation and functionality of CD4 T cells induced by the ESX-1 vaccine (not sharing Ags with BCG). The ESX-1 vaccine–specific T cells retained their differentiation status after *M. tuberculosis* infection, and their ability to enter the infected lung parenchyma was increased compared with the T cells in the H65-boosted group. As a result, the ESX-1 vaccine significantly augmented an already strong BCG-induced protection, and we obtained 1.8–2.9 $\log_{10}$ reduction in the lung bacterial load. Importantly, the BCG-priming vaccine was administered more than 6 mo prior to subunit vaccination, suggesting that it was the BCG "T cell imprint," rather than ongoing bacterial multiplication, that influenced the response of the subunit booster vaccine. In other words, the BCG-specific CD4 T cells appeared to be "locked" with minimal capacity for reprograming into potentially more favorable phenotypes 6 mo later. This is likely because highly differentiated Th1 cells exhibit limited functional plasticity (42, 43) and that subunit boosting merely expands the existing pool (or a subset) of BCG-imprinted CD4 T cells. In addition, BCG may also induce a specific regulatory T cell response that could influence booster vaccines, although this was not investigated in this study (44, 45). Regardless, de novo priming of CD4 T cells using ESX-1–associated (or other *M. tuberculosis*–specific) Ags bypass this issue, which could be a useful strategy to increase durable protection in BCG-vaccinated populations. A limitation of this study was a lack of specific homing-related makers in the analysis, and in future studies, it will be important to establish whether vaccine-induced reduction of T cell differentiation leads to increased expression of such markers and/or increased contact between Ag-specific CD4 T cells and *M. tuberculosis*–infected macrophages in the lung.

The mouse model has been extensively used to evaluate new prime–boost strategies using *M. bovis* BCG and subunit vaccines. The results have varied from no additional protection to almost 2 $\log_{10}$ protection compared with the BCG control group (46–48). It is difficult to do a comparative evaluation of these results as the studies differ with regard to vaccine design, mouse strain, *M. tuberculosis* challenge strain, BCG strain, and dose as well as the interval between prime–boost, boost–challenge, and challenge–sacrifice. However, by evaluating eight different available studies with BCG booster vaccines, we observed that the added protection of BCG boosting only was significant when the BCG-induced protection in itself was low (<0.5 $\log_{10}$) (47, 49–55). In light of our results, one explanation for this could be that a poor BCG vaccine take (or a waning response) will open up for better priming of less differentiated T cell response by the subunit vaccine. In humans, BCG will in most cases be administered to infants, and future booster vaccines are intended to be administered 10–15 y later and preferably before the protective efficacy of BCG wanes. It is not clear how pre-existing BCG immunity will influence subunit vaccination in this setting, and exposure to *M. tuberculosis* is also likely to play a dominant role in high-endemic areas. In this regard, results demonstrating that subunit vaccines can build on pre-existing *M. tuberculosis* immunity have been obtained in the recent phase IIb trial, in which M72/AS01e induced 49.7% vaccine efficacy against pulmonary disease in quantiferon positive individuals after 3 y of follow-up (56). Encouragingly, in this study, we also demonstrate that H74 vaccination significantly reduced bacterial burden in the modified Cornell model of postexposure vaccination. Similarly, regarding BCG-vaccinated quantiferon negative individuals, a recent study showed that it is possible to boost BCG protection with a subunit vaccine in adolescents and adults to some extent (57). In this study, H4:IC31 boosting led to 30.1% vaccine efficacy against sustained quantiferon conversion, and based on our data, we speculate that subunit vaccines with ESX-1–associated Ags have

the potential to further improve on this result. Additionally, in the study by Nemes et al., BCG revaccination showed a vaccine efficacy of 40.5%, which has sparked renewed interest in using BCG revaccination as a readily applicable intervention (58). In such settings, the influence of recent "BCG imprinting" is likely to be significantly higher if BCG revaccination is to be combined with future subunit vaccines.

In conclusion, mycobacterial priming by BCG vaccination induces highly differentiated CD4 T cells that, for at least 6 mo in the mouse model, restrict subsequent booster vaccines in priming additional protective T cells with sufficient memory and lung-homing potential. This phenomenon can efficiently be bypassed by designing vaccines with *M. tuberculosis*–specific Ags, like the ESX-1–associated Ags studied in this report. We suggest that future studies explore these findings in the human setting, in which it could also be investigated whether exposure to non-tuberculousis mycobacteria play a role in maintaining BCG immunity/T cell "imprint."

Acknowledgments

We thank Joshua Woodworth for input on data interpretation and gratefully acknowledge Vivi Andersen and Camilla Rasmussen at Statens Serum Institut for excellent technical assistance.

Disclosures

C.A., N.P.H.K., I.S., E.H.K., T.L., E.M.A., M.R., I.R., P.A., and R.M. are employed by Statens Serum Institut, a nonprofit government research facility of which H56, H64, and H74 and the CAF01 adjuvant are proprietary products. C.A., P.A., and R.M. are coinventors of patents covering ESX-1–based vaccines.

References

1. WHO. 2018. *Global Tuberculosis Report 2018.* World Health Organization, Geneva, Switzerland.
2. Trunz, B. B., P. Fine, and C. Dye. 2006. Effect of BCG vaccination on childhood tuberculous meningitis and miliary tuberculosis worldwide: a meta-analysis and assessment of cost-effectiveness. *Lancet* 367: 1173–1180.
3. Mangtani, P., I. Abubakar, C. Ariti, R. Beynon, L. Pimpin, P. E. M. Fine, L. C. Rodrigues, P. G. Smith, M. Lipman, P. F. Whiting, and J. A. Sterne. 2014. Protection by BCG vaccine against tuberculosis: a systematic review of randomized controlled trials. *Clin. Infect. Dis.* 58: 470–480.
4. Leveton, C., S. Barnass, B. Champion, S. Lucas, B. De Souza, M. Nicol, D. Banerjee, and G. Rook. 1989. T-cell-mediated protection of mice against virulent *Mycobacterium tuberculosis*. *Infect. Immun.* 57: 390–395.
5. Green, A. M., R. Difazio, and J. L. Flynn. 2013. IFN-γ from CD4 T cells is essential for host survival and enhances CD8 T cell function during Mycobacterium tuberculosis infection. *J. Immunol.* 190: 270–277.
6. Moguche, A. O., M. Musvosvi, A. Penn-Nicholson, C. R. Plumlee, H. Mearns, H. Geldenhuys, E. Smit, D. Abrahams, V. Rozot, O. Dintwe, et al. 2017. Antigen availability shapes T cell differentiation and function during tuberculosis. *Cell Host Microbe* 21: 695–706.e5.
7. Sallin, M. A., S. Sakai, K. D. Kauffman, H. A. Young, J. Zhu, and D. L. Barber. 2017. Th1 differentiation drives the accumulation of intravascular, non-protective CD4 T cells during tuberculosis. *Cell Rep.* 18: 3091–3104.
8. He, H., P. N. Nehete, B. Nehete, E. Wieder, G. Yang, S. Buchl, and K. J. Sastry. 2011. Functional impairment of central memory CD4 T cells is a potential early prognostic marker for changing viral load in SHIV-infected rhesus macaques. *PLoS One* 6: e19607.
9. Sakai, S., K. D. Kauffman, J. M. Schenkel, C. C. McBerry, K. D. Mayer-Barber, D. Masopust, and D. L. Barber. 2014. Cutting edge: control of *Mycobacterium tuberculosis* infection by a subset of lung parenchyma-homing CD4 T cells. *J. Immunol.* 192: 2965–2969.
10. Srivastava, S., and J. D. Ernst. 2013. Cutting edge: direct recognition of infected cells by CD4 T cells is required for control of intracellular *Mycobacterium tuberculosis* in vivo. *J. Immunol.* 191: 1016–1020.
11. Lindenstrøm, T., A. Moguche, M. Damborg, E. M. Agger, K. Urdahl, and P. Andersen. 2018. T cells primed by live mycobacteria versus a tuberculosis subunit vaccine exhibit distinct functional properties. *EBioMedicine* 27: 27–39.
12. Perdomo, C., U. Zedler, A. A. Kühl, L. Lozza, P. Saikali, L. E. Sander, A. Vogelzang, S. H. E. Kaufmann, and A. Kupz. 2016. Mucosal BCG vaccination induces protective lung-resident memory T cell populations against tuberculosis. *mBio* 7: e01686-16.
13. Orme, I. M. 2010. The Achilles heel of BCG. *Tuberculosis (Edinb.)* 90: 329–332.
14. Rodo, M. J., V. Rozot, E. Nemes, O. Dintwe, M. Hatherill, F. Little, and T. J. Scriba. 2019. A comparison of antigen-specific T cell responses induced by six novel tuberculosis vaccine candidates. *PLoS Pathog.* 15: e1007643.
15. Woodworth, J. S., S. B. Cohen, A. O. Moguche, C. R. Plumlee, E. M. Agger, K. B. Urdahl, and P. Andersen. 2017. Subunit vaccine H56/CAF01 induces a population of circulating CD4 T cells that traffic into the *Mycobacterium tuberculosis*-infected lung. *Mucosal Immunol.* 10: 555–564.
16. Hoang, T., C. Aagaard, J. Dietrich, J. P. Cassidy, G. Dolganov, G. K. Schoolnik, C. V. Lundberg, E. M. Agger, and P. Andersen. 2013. ESAT-6 (EsxA) and TB10.4 (EsxH) based vaccines for pre- and post-exposure tuberculosis vaccination. *PLoS One* 8: e80579.
17. Billeskov, R., T. Lindenstrøm, J. Woodworth, C. Vilaplana, P. J. Cardona, J. P. Cassidy, R. Mortensen, E. M. Agger, and P. Andersen. 2018. High antigen dose is detrimental to post-exposure vaccine protection against tuberculosis. *Front. Immunol.* 8: 1973.
18. Henao-Tamayo, M., G. S. Palaniswamy, E. E. Smith, C. A. Shanley, B. Wang, I. M. Orme, R. J. Basaraba, N. M. DuTeau, and D. Ordway. 2009. Post-exposure vaccination against *Mycobacterium tuberculosis*. *Tuberculosis (Edinb.)* 89: 142–148.
19. Turner, J., E. R. Rhoades, M. Keen, J. T. Belisle, A. A. Frank, and I. M. Orme. 2000. Effective preexposure tuberculosis vaccines fail to protect when they are given in an immunotherapeutic mode. *Infect. Immun.* 68: 1706–1709.
20. Taylor, J. L., O. C. Turner, R. J. Basaraba, J. T. Belisle, K. Huygen, and I. M. Orme. 2003. Pulmonary necrosis resulting from DNA vaccination against tuberculosis. *Infect. Immun.* 71: 2192–2198.
21. Knudsen, N. P., S. Nørskov-Lauritsen, G. M. Dolganov, G. K. Schoolnik, T. Lindenstrøm, P. Andersen, E. M. Agger, and C. Aagaard. 2014. Tuberculosis vaccine with high predicted population coverage and compatibility with modern diagnostics. *Proc. Natl. Acad. Sci. USA* 111: 1096–1101.
22. Aguilo, N., J. Gonzalo-Asensio, S. Alvarez-Arguedas, D. Marinova, A. B. Gomez, S. Uranga, R. Spallek, M. Singh, R. Audran, F. Spertini, and C. Martin. 2017. Reactogenicity to major tuberculosis antigens absent in BCG is linked to improved protection against *Mycobacterium tuberculosis*. *Nat. Commun.* 8: 16085.
23. Pym, A. S., P. Brodin, L. Majlessi, R. Brosch, C. Demangel, A. Williams, K. E. Griffiths, G. Marchal, C. Leclerc, and S. T. Cole. 2003. Recombinant BCG exporting ESAT-6 confers enhanced protection against tuberculosis. *Nat. Med.* 9: 533–539.
24. Gröschel, M. I., F. Sayes, S. J. Shin, W. Frigui, A. Pawlik, M. Orgeur, R. Canetti, N. Honoré, R. Simeone, T. S. van der Werf, et al. 2017. Recombinant BCG expressing ESX-1 of *Mycobacterium* marinum combines low virulence with cytosolic immune signaling and improved TB protection. *Cell Rep.* 18: 2752–2765.
25. Bottai, D., W. Frigui, S. Clark, E. Rayner, A. Zelmer, N. Andreu, M. I. de Jonge, G. J. Bancroft, A. Williams, P. Brodin, and R. Brosch. 2015. Increased protective efficacy of recombinant BCG strains expressing virulence-neutral proteins of the ESX-1 secretion system. *Vaccine* 33: 2710–2718.
26. Aagaard, C. S., T. T. Hoang, C. Vingsbo-Lundberg, J. Dietrich, and P. Andersen. 2009. Quality and vaccine efficacy of CD4+ T cell responses directed to dominant and subdominant epitopes in ESAT-6 from *Mycobacterium tuberculosis*. *J. Immunol.* 183: 2659–2668.
27. Aagaard, C., T. Hoang, J. Dietrich, P. J. Cardona, A. Izzo, G. Dolganov, G. K. Schoolnik, J. P. Cassidy, R. Billeskov, and P. Andersen. 2011. A multistage tuberculosis vaccine that confers efficient protection before and after exposure. *Nat. Med.* 17: 189–194.
28. Cole, S. T., R. Brosch, J. Parkhill, T. Garnier, C. Churcher, D. Harris, S. V. Gordon, K. Eiglmeier, S. Gas, C. E. Barry, III, et al. 1998. Deciphering the biology of *Mycobacterium tuberculosis* from the complete genome sequence. *Nature* 393: 537–544.
29. Behr, M. A., M. A. Wilson, W. P. Gill, H. Salamon, G. K. Schoolnik, S. Rane, and P. M. Small. 1999. Comparative genomics of BCG vaccines by whole-genome DNA microarray. *Science* 284: 1520–1523.
30. Millington, K. A., S. M. Fortune, J. Low, A. Garces, S. M. Hingley-Wilson, M. Wickremasinghe, O. M. Kon, and A. Lalvani. 2011. Rv3615c is a highly immunodominant RD1 (region of difference 1)-dependent secreted antigen specific for *Mycobacterium tuberculosis* infection. *Proc. Natl. Acad. Sci. USA* 108: 5730–5735.
31. van Pinxteren, L. A., P. Ravn, E. M. Agger, J. Pollock, and P. Andersen. 2000. Diagnosis of tuberculosis based on the two specific antigens ESAT-6 and CFP10. *Clin. Diagn. Lab. Immunol.* 7: 155–160.
32. Coscolla, M., and S. Gagneux. 2010. Does *M. tuberculosis* genomic diversity explain disease diversity? *Drug Discov. Today Dis. Mech.* 7: e43–e59.
33. Manca, C., L. Tsenova, S. Freeman, A. K. Barczak, M. Tovey, P. J. Murray, C. Barry, and G. Kaplan. 2005. Hypervirulent *M. tuberculosis* W/Beijing strains upregulate type I IFNs and increase expression of negative regulators of the Jak-Stat pathway. *J. Interferon Cytokine Res.* 25: 694–701.
34. Nandakumar, S., S. Kannanganat, J. E. Posey, R. R. Amara, and S. B. Sable. 2014. Attrition of T-cell functions and simultaneous upregulation of inhibitory markers correspond with the waning of BCG-induced protection against tuberculosis in mice. *PLoS One* 9: e113951.
35. Seder, R. A., P. A. Darrah, and M. Roederer. 2008. T-cell quality in memory and protection: implications for vaccine design. [Published erratum appears in 2008 *Nat. Rev. Immunol.* 8: 486.] *Nat. Rev. Immunol.* 8: 247–258.
36. McCune, R. M., Jr., W. McDermott, and R. Tompsett. 1956. The fate of *Mycobacterium tuberculosis* in mouse tissues as determined by the microbial enumeration technique. II. The conversion of tuberculous infection to the latent state by the administration of pyrazinamide and a companion drug. *J. Exp. Med.* 104: 763–802.

37. Sakai, S., K. D. Mayer-Barber, and D. L. Barber. 2014. Defining features of protective CD4 T cell responses to *Mycobacterium tuberculosis*. *Curr. Opin. Immunol.* 29: 137–142.
38. Lewinsohn, D. A., D. M. Lewinsohn, and T. J. Scriba. 2017. Polyfunctional $CD4^+$ T cells as targets for tuberculosis vaccination. *Front. Immunol.* 8: 1262.
39. Glynn, J. R., J. Whiteley, P. J. Bifani, K. Kremer, and D. van Soolingen. 2002. Worldwide occurrence of Beijing/W strains of *Mycobacterium tuberculosis*: a systematic review. *Emerg. Infect. Dis.* 8: 843–849.
40. Caws, M., G. Thwaites, K. Stepniewska, T. N. Nguyen, T. H. Nguyen, T. P. Nguyen, N. T. Mai, M. D. Phan, H. L. Tran, T. H. Tran, et al. 2006. Beijing genotype of *Mycobacterium tuberculosis* is significantly associated with human immunodeficiency virus infection and multidrug resistance in cases of tuberculous meningitis. *J. Clin. Microbiol.* 44: 3934–3939.
41. Ordway, D. J., S. Shang, M. Henao-Tamayo, A. Obregon-Henao, L. Nold, M. Caraway, C. A. Shanley, R. J. Basaraba, C. G. Duncan, and I. M. Orme. 2011. *Mycobacterium* bovis BCG-mediated protection against W-Beijing strains of *Mycobacterium tuberculosis* is diminished concomitant with the emergence of regulatory T cells. *Clin. Vaccine Immunol.* 18: 1527–1535.
42. Zhu, J., and W. E. Paul. 2010. Heterogeneity and plasticity of T helper cells. *Cell Res.* 20: 4–12.
43. Geginat, J., M. Paroni, S. Maglie, J. S. Alfen, I. Kastirr, P. Gruarin, M. De Simone, M. Pagani, and S. Abrignani. 2014. Plasticity of human CD4 T cell subsets. *Front. Immunol.* 5: 630.
44. Chevalier, M. F., A. K. Schneider, V. Cesson, F. Dartiguenave, I. Lucca, P. Jichlinski, D. Nardelli-Haefliger, and L. Derré. 2018. Conventional and PD-L1-expressing regulatory T cells are enriched during BCG therapy and may limit its efficacy. *Eur. Urol.* 74: 540–544.
45. de Cassan, S. C., A. A. Pathan, C. R. Sander, A. Minassian, R. Rowland, A. V. Hill, H. McShane, and H. A. Fletcher. 2010. Investigating the induction of vaccine-induced Th17 and regulatory T cells in healthy, *Mycobacterium* bovis BCG-immunized adults vaccinated with a new tuberculosis vaccine, MVA85A. *Clin. Vaccine Immunol.* 17: 1066–1073.
46. Brennan, M. J., B. Clagett, H. Fitzgerald, V. Chen, A. Williams, A. A. Izzo, and L. F. Barker. 2012. Preclinical evidence for implementing a prime-boost vaccine strategy for tuberculosis. *Vaccine* 30: 2811–2823.
47. Brandt, L., Y. A. Skeiky, M. R. Alderson, Y. Lobet, W. Dalemans, O. C. Turner, R. J. Basaraba, A. A. Izzo, T. M. Lasco, P. L. Chapman, et al. 2004. The protective effect of the *Mycobacterium* bovis BCG vaccine is increased by coadministration with the *Mycobacterium tuberculosis* 72-kilodalton fusion polyprotein Mtb72F in *M. tuberculosis*-infected guinea pigs. *Infect. Immun.* 72: 6622–6632.
48. Billeskov, R., T. T. Elvang, P. L. Andersen, and J. Dietrich. 2012. The HyVac4 subunit vaccine efficiently boosts BCG-primed anti-mycobacterial protective immunity. *PLoS One* 7: e39909.
49. Tchilian, E. Z., C. Desel, E. K. Forbes, S. Bandermann, C. R. Sander, A. V. Hill, H. McShane, and S. H. Kaufmann. 2009. Immunogenicity and protective efficacy of prime-boost regimens with recombinant (delta)ureC hly+ *Mycobacterium* bovis BCG and modified vaccinia virus ankara expressing *M. tuberculosis* antigen 85A against murine tuberculosis. *Infect. Immun.* 77: 622–631.
50. Romano, M., S. D'Souza, P. Y. Adnet, R. Laali, F. Jurion, K. Palfliet, and K. Huygen. 2006. Priming but not boosting with plasmid DNA encoding mycolyl-transferase Ag85A from *Mycobacterium tuberculosis* increases the survival time of *Mycobacterium* bovis BCG vaccinated mice against low dose intravenous challenge with *M. tuberculosis* H37Rv. *Vaccine* 24: 3353–3364.
51. da Fonseca, D. M., C. L. Silva, P. F. Wowk, M. O. E. Paula, S. G. Ramos, C. Horn, G. Marchal, and V. L. D. Bonato. 2009. *Mycobacterium tuberculosis* culture filtrate proteins plus CpG Oligodeoxynucleotides confer protection to *Mycobacterium bovis* BCG-primed mice by inhibiting interleukin-4 secretion. *Infect. Immun.* 77: 5311–5321.
52. Rahman, M. J., and C. Fernández. 2009. Neonatal vaccination with *Mycobacterium* bovis BCG: potential effects as a priming agent shown in a heterologous prime-boost immunization protocol. *Vaccine* 27: 4038–4046.
53. Haile, M., B. Hamasur, T. Jaxmar, D. Gavier-Widen, M. A. Chambers, B. Sanchez, U. Schröder, G. Källenius, S. B. Svenson, and A. Pawlowski. 2005. Nasal boost with adjuvanted heat-killed BCG or arabinomannan-protein conjugate improves primary BCG-induced protection in C57BL/6 mice. *Tuberculosis (Edinb.)* 85: 107–114.
54. Mollenkopf, H. J., L. Grode, J. Mattow, M. Stein, P. Mann, B. Knapp, J. Ulmer, and S. H. Kaufmann. 2004. Application of mycobacterial proteomics to vaccine design: improved protection by *Mycobacterium* bovis BCG prime-Rv3407 DNA boost vaccination against tuberculosis. *Infect. Immun.* 72: 6471–6479.
55. Majlessi, L., M. Simsova, Z. Jarvis, P. Brodin, M. J. Rojas, C. Bauche, C. Nouzé, D. Ladant, S. T. Cole, P. Sebo, and C. Leclerc. 2006. An increase in antimycobacterial Th1-cell responses by prime-boost protocols of immunization does not enhance protection against tuberculosis. *Infect. Immun.* 74: 2128–2137.
56. Tait, D. R., M. Hatherill, O. Van Der Meeren, A. M. Ginsberg, E. Van Brakel, B. Salaun, T. J. Scriba, E. J. Akite, H. M. Ayles, A. Bollaerts, et al. 2019. Final analysis of a trial of $M72/AS01_E$ vaccine to prevent tuberculosis. *N. Engl. J. Med.* 381: 2429–2439.
57. Nemes, E., H. Geldenhuys, V. Rozot, K. T. Rutkowski, F. Ratangee, N. Bilek, S. Mabwe, L. Makhethe, M. Erasmus, A. Toefy, et al; C-040-404 Study Team. 2018. Prevention of *M. tuberculosis* infection with H4:IC31 vaccine or BCG revaccination. *N. Engl. J. Med.* 379: 138–149.
58. Andersen, P., and T. J. Scriba. 2019. Moving tuberculosis vaccines from theory to practice. *Nat. Rev. Immunol.* 19: 550–562.
59. Målen, H., S. Pathak, T. Søfteland, G. A. de Souza, and H. G. Wiker. 2010. Definition of novel cell envelope associated proteins in Triton X-114 extracts of *Mycobacterium tuberculosis* H37Rv. *BMC Microbiol.* DOI: 10.1186/1471-2180-10-132.
60. de Souza, G. A., M. Ø. Arntzen, S. Fortuin, A. C. Schürch, H. Målen, C. R. E. McEvoy, D. van Soolingen, B. Thiede, R. M. Warren, and H. G. Wiker. 2011. Proteogenomic analysis of polymorphisms and gene annotation divergences in prokaryotes using a clustered mass spectrometry-friendly database. Mol. Cell Proteomics. DOI: 10.1074/mcp.M110.002527.